# Characterization of a new G-type halohydrin dehalogenase with enhanced catalytic activity

Sophie Günther, Anett Schallmey*

Sophie Günther, Prof. Dr. Anett Schallmey

Institute for Biochemistry, Biotechnology and Bioinformatics, Technische Universität Braunschweig, Spielmannstr. 7, 38106 Braunschweig, Germany

* **Correspondance**

Prof. Dr. Anett Schallmey

Email: a.schallmey@tu-braunschweig.de

Halohydrin dehalogenases (HHDHs) (E.C.4.5.1.-) are bacterial lyases belonging to the superfamily of short-chain dehydrogenases/reductases (SDR).[1] They catalyze the reversible dehalogenation of vicinal haloalcohols with epoxide formation. In the reverse reaction, i.e. epoxide ring opening, a variety of nucleophiles are accepted enabling the formation of new C-C, C-O, C-N and C-S bonds.[2] Halohydrin dehalogenase HheG from *Ilumatobacter coccineus* was previously found to accept also sterically more demanding cyclic epoxides as well as acyclic non-terminal epoxide substrates.[3,4] This special feature is based on HheG's broader active site compared to other structurally characterized HHDHs.[3,5,6] We herein report the biochemical characterization of a new HheG homolog, HheG-682 from *Actinobacteria bacterium*, which has been identified via BLAST search in the nr protein sequence database of GenBank.

Initially, HheG-682 (GenBank: PHX59682) was heterologously produced in *Escherichia coli* BL21(DE3) from pET28a(+) resulting in an N-terminal $His_6$-tagged protein. Afterwards, HheG-682 was purified via immobilized metal ion affinity chromatography (IMAC) based on established protocols.[7] This yielded 156 mg HheG-682 per liter expression culture, which is similar to the respective yield for HheG.

Epoxide ring opening activity of HheG-682 towards six different epoxides (Scheme 1) was determined in reactions using each 10 mM epoxide, 20 mM azide as nucleophile and 50 µg $mL^{-1}$ of purified enzyme. For comparison, reactions using HheG instead of HheG-682, as well as negative control reactions without enzyme addition were performed in parallel. Reactions were analyzed by achiral GC using previously published protocols.[3,7–9] Reactions with cyclohexene oxide (**7**) were further measured on chiral GC as previously described[3,7,8] to determine the enantiomeric excess of formed azidoalcohol **8**. Compared to HheG, HheG-682 displayed significantly (up to 4-fold) higher conversion after 1 h for five of the six epoxide substrates (Figure 1). Only epoxide **1** is hardly converted by both HHDHs. Apart from that, no significant difference in the enantioselectivity of both enzymes for epoxide ring opening of cyclohexene oxide (**7**) with azide could be observed. Both HHDHs preferentially formed (1*S*,2*S*)-2-azido-1-cyclohexanol (**8b**) in similar enantiomeric excess ($ee_p$=49.9 % for HheG and 52.4 % for HheG-682).

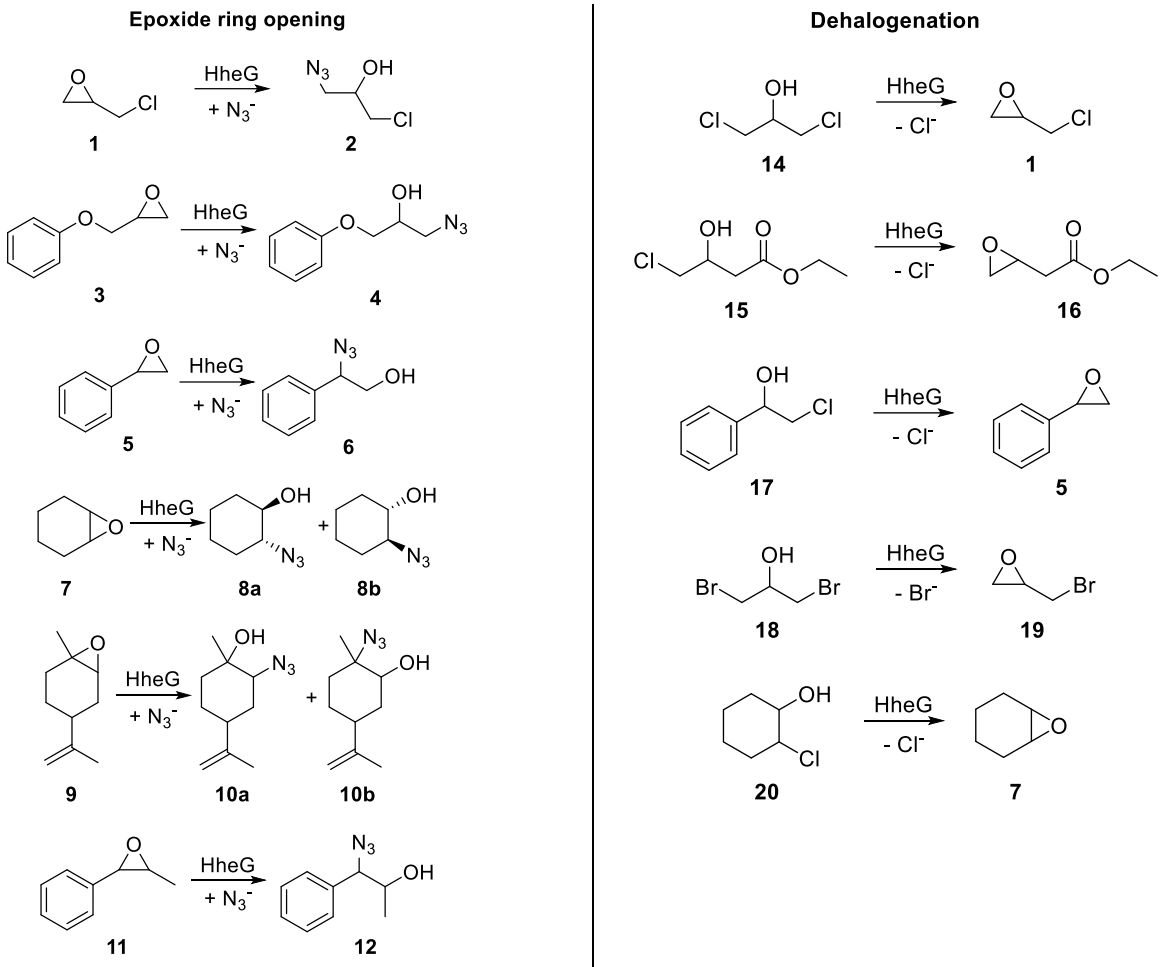


**Scheme 1:** Epoxide ring opening and dehalogenation reactions of HheG and HheG-682 performed in this study [**1**: epichlorohydrin, **2**: 1-azido-3-chloro-2-propanol, **3:** phenylglycidylether, **4:** 1-azido-3-phenoxy-propan-2-ol, **5:** styrene oxide, **6:** 2-azido-2-phenylethanol, **7:** cyclohexene oxide, **8a:** (1*R*,2*R*)-2-azido-1-cyclohexanol, **8b:** (1*S*,2*S*)-2-azido-1-cyclohexanol, **9:** (+)-*cis/trans*-limonene oxide, **10a:** 2-azido-1-methyl-4-(prop-1-en-2-yl)cyclohexan-1-ol, **10b:** 2-azido-2-methyl-5-(prop-1-en-2-yl) cyclohexan-1-ol, **11:** *trans*-1-phenylpropylene oxide, **12:** 1-azido-1-phenylpropan-2-ol, **14**: 1,3-dichloro-2-propanol, **15:** ethyl-4-chloro-3-hydroxybutyrate, **16:** ethyl 2-(oxiran-2-yl)acetate, **17:** 2-chloro-1-phenylethanol, **18:** 1,3-dibromo-2-propanol, **19:** epibromohydrin, **20:** 2-chlorocyclohexanol].

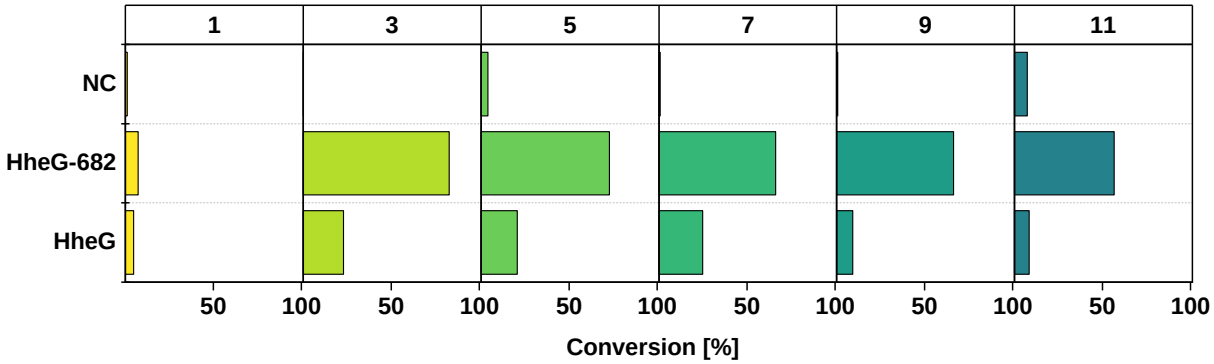


**Figure 1:** Conversions of 10 mM epoxide substrates epichlorohydrin (**1**), phenylglycidylether (**3**), styrene oxide (**5**), cyclohexene oxide (**7**), (+)-*cis/trans*-limonene oxide (**9**) and *trans*-1-phenylpropylene oxide (**11**) with 20 mM azide in 50 mM Tris·$SO_4$, pH 7.0, at 30 °C and 900 rpm using 50 µg $mL^{-1}$ purified HheG or HheG-682. Reactions were carried out in a total of 1 mL. Samples were taken after 24 h for epoxide **1** or after 1 h in case of epoxides **3**, **5**, **7**, **9** and **11**, extracted with an equal volume *tert*-butyl methyl ether and analyzed by achiral GC. "NC" represents negative control reactions without enzyme addition.

Additionally, specific activities based on initial reaction velocities of HheG and HheG-682 in the azidolysis of the different epoxide substrates were determined using an adapted, pH-based spectrophotometric assay.[10] Reactions were performed at 30°C using 10 mM epoxide, 20 mM azide and 100 µg $mL^{-1}$ purified enzyme. As expected, both HheG and HheG-682 displayed low specific activity with epoxide **1** (Figure 2), while for all other tested epoxides the specific activities of HheG-682 were significantly higher compared to HheG. The highest (13.6-fold) increase in specific activity was obtained with epoxide **11**. Hence, HheG-682 is significantly more active, especially also with the sterically more demanding substrates **7**, **9** and **11**, than HheG.

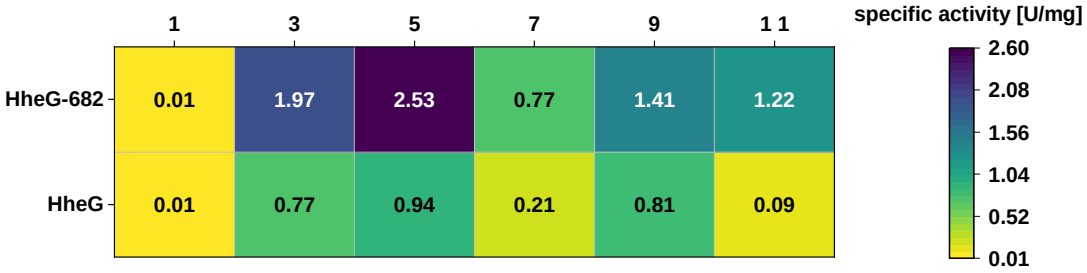


**Figure 2:** Specific activities (U $mg^{-1}$) based on initial reaction rates of HheG and HheG-682 in epoxide ring opening of epoxides epichlorohydrin (**1**), phenylglycidylether (**3**), styrene oxide (**5**), cyclohexene oxide (**7**), (+)-*cis/trans*-limonene oxide (**9**) and *trans*-1-phenylpropylene oxide (**11**) determined with a spectrophotometric assay.[10] Reactions were carried out in duplicate in a total volume of 1 mL with 10 mM epoxide and 20 mM azide in 2 mM buffer at 30 °C using 100 µg $mL^{-1}$ purified enzyme. Samples

were taken after 30, 60, 180, 270 and 360 s and quenched in equal volumes of MeOH. Chemical background of negative control reactions without enzyme addition were subtracted. Resulting specific activities exhibit standard deviations between 0.0 and 0.1 U $mg^{-1}$.

Moreover, HheG-682's activity in terms of conversion was also studied with other HHDH-typical nucleophiles in the epoxide ring opening of phenylglycidylether (**3**) and compared to HheG (Figure 3). This revealed a potentially better acceptance of the nucleophiles nitrite, chloride and cyanate by HheG-682, as significantly higher conversions were obtained for this enzyme in comparison to HheG.

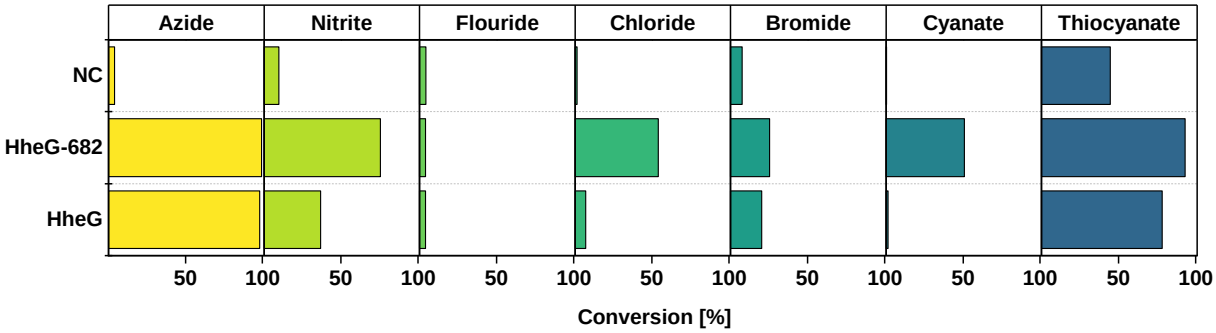


**Figure 3:** Conversions of 10 mM phenylglycidylether (**3**) with 20 mM of different nucleophiles in 50 mM Tris·$SO_4$, pH 7.0, at 30 °C using 150 µg $mL^{-1}$ purified HheG or HheG-682. Reactions were carried out in a total of 1 mL. Samples were taken after 24 h, extracted with an equal volume of *tert*-butyl methyl ether and analyzed by achiral GC.

Apart from epoxide ring opening, specific activities of HheG-682 in comparison to HheG were further determined in the dehalogenation of 1,3-dichloro-2-propanol (**14**), ethyl-4-chloro-3-hydroxybutyrate (**15**), ethyl 2-(oxiran-2-yl)acetate (**16**), 2-chloro-1-phenylethanol (**17**), 1,3-dibromo-2-propanol (**18**) and 2-chlorocyclohexanol (**20**) (Scheme 1) using the spectrophotometric halide release assay.[9,11] As shown in Figure 4, HheG-682 is slightly more active than HheG in the dehalogenation of haloalcohols **14**, **15** and **18**, whereas an almost 10-fold higher specific activity was obtained with haloalcohol **20**. Therefore, also kinetic parameters of HheG-682 in the dehalogenation of 2-chlorocyclohexanol (**20**) were determined and compared to respective literature data for HheG (Table 1).[3] This revealed a 5.2-times higher $k_{cat}$ of HheG-682, while the $K_{50}$ was also increased two-fold, resulting in an overall higher catalytic efficiency of HheG-682 in the dehalogenation of **20** compared to HheG. Interestingly, both enzymes displayed strong cooperativity for binding of haloaclohol **20** with Hill coefficients of 2.9 and 3.2 for HheG and HheG-682, respectively.

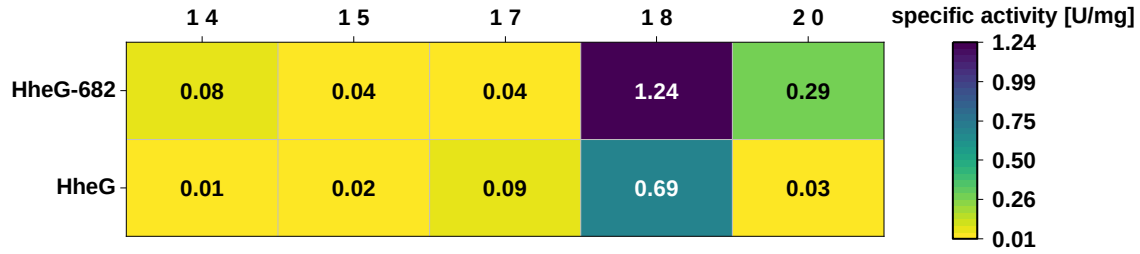


**Figure 4:** Specific activities (U $mg^{-1}$) based on initial rates of HheG and HheG-682 in the dehalogenation of haloalcohols 1,3-dichloro-2-propanol (**14**), ethyl-4-chloro-3-hydroxybutyrate (**15**), ethyl 2-(oxiran-2-yl)acetate (**16**), 2-chloro-1-phenylethanol (**17**), 1,3-dibromo-2-propanol (**18**) and 2-chlorocyclohexanol (**20**) determined with a halide release assay.[9,11] Reactions were carried out in a total volume of 1 mL with 10 mM haloalcohol in 25 mM Tris·$SO_4$ buffer, pH 7.0, at 30 °C using either 200 µg $mL^{-1}$ HheG or 150 µg $mL^{-1}$ HheG-682. Samples were taken after 30, 60, 90, 120, 150, 180 s as duplicates. Chemical background of negative control reactions without enzyme addition was subtracted. The resulting specific activities exhibit standard deviations between 0.0 and 0.2 U $mg^{-1}$.

**Table 1:** Comparison of kinetic parameters of HheG and HheG-682 for the dehalogenation of 2-chlorocyclohexanol (**20**). Reactions were carried out in a total volume of 1 mL with 1–150 mM haloalcohol in the presence of 2% DMSO in 25 mM Tris·$SO_4$ buffer, pH 7.0, at 30 °C using 150 µg $mL^{-1}$ HheG-682. Samples were taken after 30, 60, 90, 120, 150, 180 s as duplicates. Chemical background of negative control reactions without enzyme addition was subtracted. The Hill equation was used for data fitting in OriginPro. Kinetic parameters for HheG were taken from Koopmeiners et al.[3]

| Enzyme | $K_{50}$ [mM] | $k_{cat}$ [$s^{-1}$] | $k_{cat}/K_{50}$ [$mM^{-1}$ $s^{-1}$] | $n_H$ |
|---|---|---|---|---|
| HheG [3] | 30.0 ± 3.0 | 0.3 ± 0.03 | 0.01 ± 0.01 | 2.9 ± 0.6 |
| HheG-682 | 65.8 ± 1.3 | 1.6 ± 0.03 | 0.03 ± 0.00 | 3.2 ± 0.2 |

HheG-682 was further characterized in terms of its apparent melting temperature ($T_m$), pH and temperature profiles, as well as oligomeric state.

Melting temperature determination was carried out according to Staar et al.[7] This revealed a 6 K higher $T_m$ for HheG-682 ($T_m$=45 °C) in comparison to HheG ($T_m$=39 °C).

The pH and temperature profiles were determined *via* the halide release assay, as described previously[9], using 10 mM haloalcohol **18** and 25 µg $mL^{-1}$ purified HheG-682. For both enzymes, the optimal pH for dehalogenation was obtained in phosphate buffer at pH 7.0 (Figure 5 A).[3] In contrast,

HheG-682 displayed its highest relative activity at 35 °C (Figure 5 B), which is 5 K higher compared to the reported highest relative activity of HheG in the dehalogenation of **18**.[3]

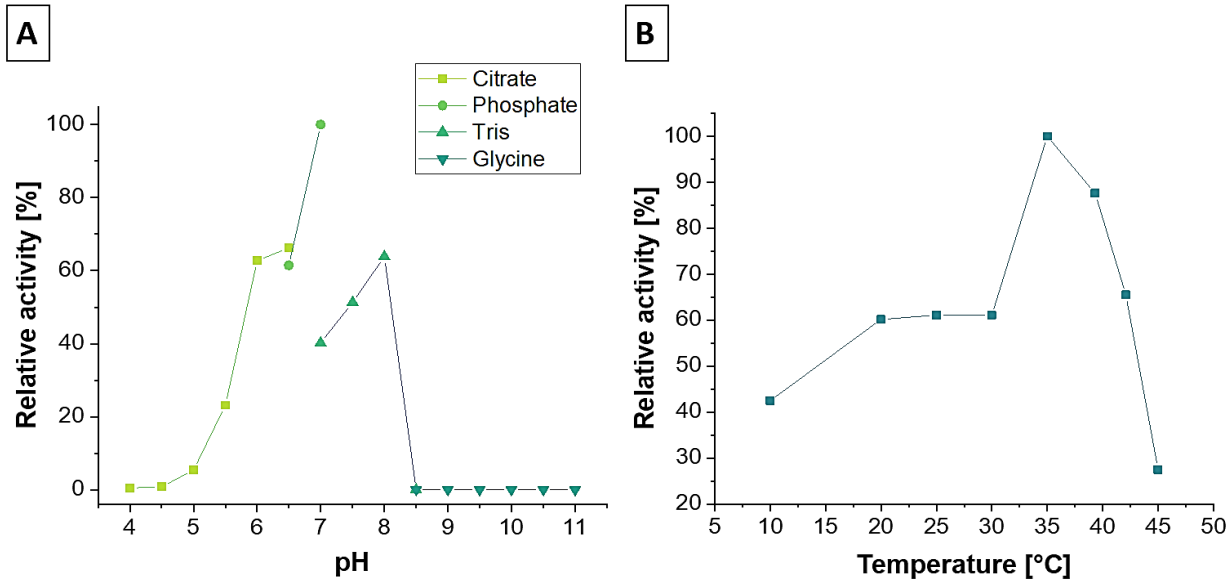


**Figure 5:** Temperature (**A**) and pH (**B**) profiles of HheG-682 in the conversion of 10 mM haloalcohol **18** using 25 µg $mL^{-1}$ purified enzyme. The reaction temperature for pH profile determination was set to 30°C. For temperature profile determination, 50 mM Tris·$SO_4$, pH 7.0 was used. Relative activities have been calculated by setting the highest obtained conversion to 100 % activity.

For determination of the oligomeric state of HheG-682 in comparison to HheG, size exclusion chromatography on a Superdex 200 Increase 10/300 GL column (GE Healthcare, Freiburg Germany) was performed using 10 mM Tris·$SO_4$ buffer, pH 7.9, containing 4 mM EDTA and 150 mM NaCl at a flow rate of 0.75 mL $min^{-1}$. After equilibration of the column, 200 µg of protein was loaded on the column and eluted again in an elution volume of 25 mL. For molecular weight determination, a protein standard mix (15-600 kDa, Sigma-Aldrich, MO USA) was run over the column under the same elution conditions. According to its crystal structure, HheG is known to exhibit a homotetrameric assembly resulting in an overall molecular mass of approx. 120 kDa (29.8 kDa per monomer).[3] As shown in Figure 6, HheG-682 and HheG displayed identical elution profiles on our SEC column, indicating also a tetrameric assembly for HheG-682. Based on the elution of the protein standard mix, a molecular weight of 133 kDa could be calculated for HheG-682, which is close to the expected 113 kDa for a homotetramer (28.3 kDa per HheG-682 monomer).

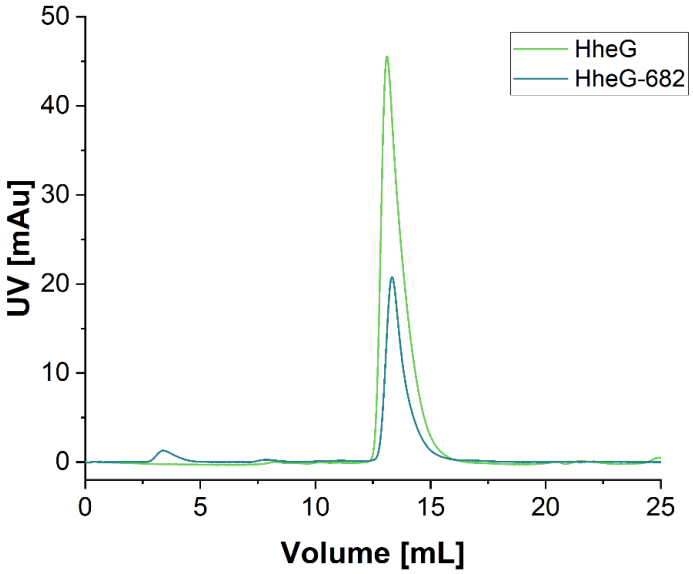


**Figure 6:** Size exclusion chromatograms of HheG (green) and HheG-682 (blue) on a Superdex 200 Increase 10/300 GL column (GE Healthcare, Freiburg Germany) using 10 mM Tris·$SO_4$ buffer, pH 7.9, containing 4 mM EDTA and 150 mM NaCl at a flow rate of 0.75 mL $min^{-1}$.

Finally, the crystal structures of HheG (PDB: 5O30)[3] and HheG-682 (PDB: 7WKQ; released by Wan, N.W.) were compared to investigate potential structural reasons for the enhanced catalytic activity of HheG-682. The overall structures of both enzymes are very similar displaying a typical Rossman fold-like architecture (Figure 7a and B). A remarkable difference, however, can be observed in the three dimensional arrangement of alpha helices α6 and α7 in HheG-682 (residues 189-212) and HheG (residues 200-223) (Figure 7B). As previously reported[3,12], residue F203 of HheG, which delimits the enzyme active site of HheG together with residues of the catalytic triad, is found in helix α6. Moreover, HheG-682 is missing the flexible loop (spanning residues 39-47 in HheG) that has been reported for HheG previously.[8] Thus, the shape and appearance of the enzyme active sites of HheG and HheG-682 show clear differences, resulting also in slight shifts of the respective catalytic residues (Figure 7 C and D). Such differences will likely explain the observed higher catalytic activity of HheG-682, but further, more detailed analyses will be necessary.

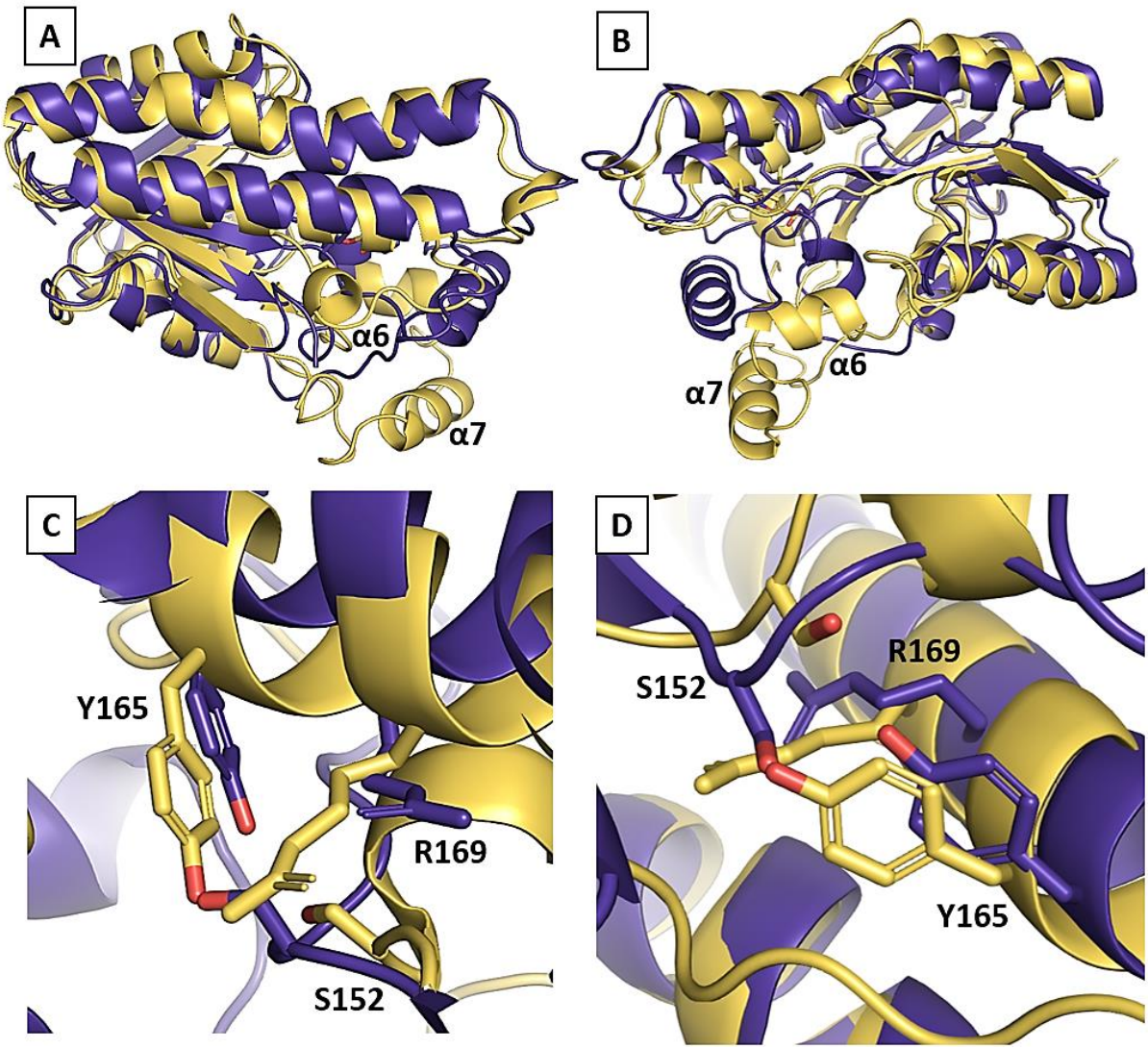


**Figure 7:** Comparison of the protein structures of HheG (PDB: 5O30, yellow) and HheG-682 (PDB: 7WKQ, violet) as an overlay of the corresponding monomers. **A+B:** Secondary structure elements within the Rossmann fold-like architecture of HheG and HheG-682 monomers. The residues constituting the catalytic triad, Ser152, Tyr165, and Arg169 (residue numbering according to HheG), are highlighted as sticks. Alpha helices α6 and α7 of HheG are highlighted. **C+D:** Close-up on the active sites of HheG and HheG-682 comprising the catalytic triad.

**References**


[1] A. Schallmey, M. Schallmey, *Appl. Microbiol. Biotechnol.* **2016**, *100*, 7827–7839.

[2] G. Hasnaoui-Dijoux, M. Majerić Elenkov, J. H. Lutje Spelberg, B. Hauer, D. B. Janssen, *ChemBioChem* **2008**, *9*, 1048–1051.

[3] J. Koopmeiners, C. Diederich, J. Solarczek, H. Voß, J. Mayer, W. Blankenfeldt, A. Schallmey, *ACS Catal.* **2017**, *7*, 6877–6886.

[4] E. Calderini, J. Wessel, P. Süss, P. Schrepfer, R. Wardenga, A. Schallmey, *ChemCatChem* **2019**, *11*, 2099–2106.

[5] R. M. de Jong, K. H. Kalk, L. Tang, D. B. Janssen, B. W. Dijkstra, *J. Bacteriol.* **2006**, *188*, 4051–4056.

[6] F. Watanabe, F. Yu, A. Ohtaki, Y. Yamanaka, K. Noguchi, M. Yohda, M. Odaka, *Proteins Struct. Funct. Bioinforma.* **2015**, *83*, 2230–2239.

[7] M. Staar, S. Henke, W. Blankenfeldt, A. Schallmey, *ChemCatChem* **2022**, DOI 10.1002/cctc.202200145.

[8] J. Solarczek, T. Klünemann, F. Brandt, P. Schrepfer, M. Wolter, C. R. Jacob, W. Blankenfeldt, A. Schallmey, *Sci. Rep.* **2019**, *9*, 5106.

[9] J. Koopmeiners, B. Halmschlag, M. Schallmey, A. Schallmey, *Appl. Microbiol. Biotechnol.* **2016**, *100*, 7517–7527.

[10] I. Gul, T. Fantaye Bogale, J. Deng, L. Wang, J. Feng, L. Tang, *J. Biotechnol.* **2020**, *311*, 19–24.

[11] M. Schallmey, J. Koopmeiners, E. Wells, R. Wardenga, A. Schallmey, *Appl. Environ. Microbiol.* **2014**, *80*, 7303–7315.

[12] J. Wessel, G. Petrillo, M. Estevez-Gay, S. Bosch, M. Seeger, W. P. Dijkman, J. Iglesias-Fernández, A. Hidalgo, I. Uson, S. Osuna, A. Schallmey, *FEBS J.* **2021**, *288*, 4683–4701.